Perfluorooctane sulfonic acid induces liver lipid accumulation through AMPK/ACC signaling

Junyi Ling
Nantong University
Lu Hua
Jiangsu Taizhou People's Hospital
Yi Qin
Nantong University
Tianye Gu
Nantong University
shengyang jiang (jiang_shengyang@163.com)
Nantong University
Jianya Zhao
Nantong University

Research Article

Keywords: PFOS, AMPK, lipid metabolism, hepatotoxicity, high-fat diet

Posted Date: May 3rd, 2022

DOI: https://doi.org/10.21203/rs.3.rs-1580546/v1

Perfluorooctane sulfonic acid induces liver lipid accumulation through AMPK/ACC signaling

Junyi Ling[1]| Lu Hua[2]| Yi Qin[1, 4]| Tianye Gu[3]| Shengyang Jiang[1]| Jianya Zhao[3]

[1]Department of Occupational Medicine and Environmental Toxicology, School of Public Health, Nantong University, Nantong, 226001, People's Republic of China
[2]Department of Oncology, Taizhou People's Hospital, Taizhou, 225300, People's Republic of China
[3]Department of Nutrition and Food Hygiene, School of Public Health, Nantong University, Nantong, 226001, People's Republic of China
[4]Haimen District Center for Disease Control and Prevention, Haimen, Nantong, 226100, People's Republic of China

Junyi Ling and Lu Hua contributed equally to this work

Corresponding Author: Shengyang Jiang (jiang_shengyang@163.com); Jianya Zhao (zhaojianya@ntu.edu.cn)

This study was supported by the National Natural Science Foundation of China (no. 81902406), Nantong Science and Technology Project (JC2020032) and Taizhou people's hospital research project (ZL201916).

Abstract

Perfluorooctane sulfonic acid (PFOS) is a hepatotoxic environmental organic pollutant that can cause aberrant lipid accumulation in the liver. However, the molecular mechanism underlying PFOS-induced hepatic steatosis remains unclear. Our research shows that low-dose PFOS exposure can inhibit AMP-activated protein kinase (AMPK) phosphorylation, leading to increased acetyl-CoA carboxylase (ACC) activity and attenuated fatty acid β-oxidation, and consequent liver lipid accumulation. We found that 1 mg/kg/day PFOS exposure significantly aggravated steatosis in high-fat diet (HFD)-fed mice, along with reduced AMPK activity. Oil Red O results showed that PFOS exposure caused fat accumulation in HepG2 cells. As predicted, PFOS treatment reduced the level of phosphorylated AMPK in a concentration-dependent manner, leading to subsequent increase in ACC activity and lipid droplet accumulation in HepG2 cells. Treatment with 200 μM AMPK agonist AICAR alleviated PFOS-induced ACC activation and lipid accumulation. In summary, our data highlights a crucial role of AMPK/ACC pathway in PFOS-mediated liver lipid metabolism disorders.

Keywords: PFOS; AMPK; lipid metabolism; hepatotoxicity; high-fat diet

INTRODUCTION

As one of the most commonly identified perfluorinated organic compounds in the environment, perfluorooctane sulfonic acid (PFOS) has been widely used in industrial and consumable fields, such as textiles, pesticides and coatings (Bach et al. 2015; Lau et al. 2004; Liu et al. 2015; Miralles-Marco and Harrad 2015).In 2009, PFOS and its related precursor chemicals were listed as new persistent organic pollutants (POPs) by the Stockholm Convention (Pollutants 2009).While its production and use have been restricted worldwide, the adverse impacts of PFOS and its precursors on the environment and organisms remain important public concerns, due to their extreme stability and bioaccumulation (Lindstrom et al. 2011).Studies have shown that PFOS has a half-life of approximate 5 years in human body (Olsen and Zobel 2007). A study indicated that perfluorinated chemicals were detectable in the serum of almost 98% of citizens in the United States and were positively associated with serum levels of uric acid, alanine transferase (ALT), gamma-glutamyl transferase (GGT) and total bilirubin (Gleason et al. 2015). Coinciding with this study, a variety of epidemiological and animal studies have shown that the main target organ for PFOS accumulation is the liver (Han et al. 2018). It has been found that mice exposed to PFOS exhibited weight loss, increased liver weight, and characteristics of hepatic steatosis (McDonough et al. 2020; Wang et al. 2014). The hepatotoxicity of PFOS is mainly featured by hepatic steatosis, hepatomegaly and increased hepatocyte proliferation. Population studies have found that PFOS concentration in the liver of general population in western countries ranges between4.7-57 ng/g (Maestri et al. 2006; Olsen et al. 2003; Perez et al. 2013). Notably, PFOS is detectable extensively in wild lives, including, and is accumulated through food chain (Giesy and Kannan 2001; Riebe et al. 2016). Meanwhile, animal studies indicated that the mice exposed to 10 mg/g/day PFOS for 21 days exhibited increased liver weight and obvious characteristics of steatohepatitis, accompanied by elevated serum levels of aspartate aminotransferase (AST), ALT, triglycerides (TG) (Huang et al. 2020; Wan et al. 2012). These studies raise a critical concern regarding a causal role of PFOS exposure on liver metabolic disorders.

The lipid metabolism in the normal liver maintains a dynamic balance of lipid

synthesis and decomposition, and when aberrantly regulated, may cause lipid accumulation in the liver and hepatic steatosis (Fang et al. 2019). The development of hepatic steatosis involves a variety of metabolic and stress signaling pathways, such as AMP-activated protein kinase (AMPK) and endoplasmic reticulum (ER) stress pathways. As a master regulator of energy and lipid metabolism, AMPK is a heterotrimeric protein, composed of three subunits: α, β, and γ. In the liver, α1 and α2 subunit isoforms are mainly expressed, and α2 is highly expressed (Herzig and Shaw 2018). In response to upstream activating stimuli, including AMP/ATP, LKB1 and CAMK, AMPK may phosphorylate and inactivate Acetyl-CoA carboxylase (ACC) to suppress fatty acid synthesis (Assifi et al. 2005; Carling et al. 1987; Munday et al. 1988). ACC has two subtypes: ACC1 and ACC2, both of which can promote the conversion of acetyl-CoA to malonyl-CoA (Lane et al. 2008). Through restoring malonyl-CoA, ACC may inhibit the activity of carnitine palmitoyl transferase-1 (CPT-1), a key enzyme for fatty acidβ-oxidation, thereby leading to reduced lipolysis (Kim et al. 2012; Schreurs et al. 2010; You et al. 2004). Dr. Pan's research found that Vitis thunbergii extract can activate AMPK, then inhibit the activation of ACC and reduce lipid accumulation in liver tissue (Pan et al. 2012). Recent animal studies have shown that AMPK may alleviate lipid accumulation in the liver to prevent the development of liver steatosis in high fat diet (HFD)-fed mice (Qiang et al. 2016). Another study has shown that increased liver triglyceride (TG) accumulation by PFOS exposure is associated with decreased level of phosphorylated AMPK (Salter et al. 2021). However, the molecular mechanisms underlying the role of AMPK in PFOS-initiated liver lipid accumulation remain unclear.

In view of the above information, we investigated the involvement of PFOS exposure on liver steatosis using HFD-induced fatty liver disease model. We found that PFOS exposure resulted in reduced expression of phosphorylated AMPK, leading to increased activity level of ACC and liver lipid accumulation. In addition, HFD promoted the accumulation of triglycerides in the liver and inhibited the phosphorylation of AMPK, which is exacerbated by PFOS exposure. We also used HepG2 cells to establish an in vitro PFOS exposure model, and found that AMPK

phosphorylation decreased in a dose-dependent manner following PFOS exposure. Meanwhile, we also observed increased accumulation of fat particles in HepG2 cells which was affected by PFOS exposure. Treatment with AMPK agonist AICAR ameliorated PFOS-induced fat accumulation. In summary, our findings indicated that AMPK/ACC pathway plays an indispensable role in PFOS-induced liver lipid accumulation and abnormal liver lipid metabolism, highlighting the importance of agonizing AMPK in the prevention of PFOS-facilitated liver steatosis.

MATERIALS AND METHODS

Chemicals

The following reagents and kits were purchased from their suppliers: Perfluorooctane sulfonate (PFOS, potassium salt, purity 98%; Sigma-Aldrich, Shanghai, China), Dimethyl sulfoxide (DMSO, Sigma, St. Louis, MO, USA), AICAR (M4869, AbMole, Shanghai, China).

Animal Model

70 male C57BL/6J mice (4 weeks old) were obtained from the Experimental Animal Center of Nantong University. All mice were kept in an environment where the ambient temperature was maintained at 20°C ± 2°C, the relative humidity was maintained at 40%-60%, and the 12 h light-dark cycle light environment was maintained, with free access to sterilized drinking water.

After one week of adaptive housing, the mice were randomly divided into two groups: normal feed diet (Chow) and high-fat feed diet (HFD; 45% of total calories from fat), and fed with the respective diets for 12weeks.In addition, each diet group was randomly divided into three groups: vehicle control (corn oil) group, 1 mg/kg PFOS group, and 5 mg/kg PFOS group. During the last four weeks of feeding, administrated daily with the vehicle control, 1 mg/kg PFOS and 5 mg/kg PFOS (0.1 ml per 10 g body weight) using oral gavage, respectively.

Body weights of the mice were recorded weekly. After a total of 12-week-feeding, the mice were fasted for 12 hours and sacrificed. The livers were resected, fixed using

4% paraformaldehyde solution and subjected to paraffin sectioning.

The above experimental protocol has been approved by the Laboratory Animal Care and Welfare Ethics Committee of Nantong University, and is strictly implemented in accordance with the National Institutes of Health Laboratory Animal Care and Use Guidelines.

Determination of Serum Alanine Aminotransferase (ALT) and Aspartate Aminotransferase (AST)

The collected blood samples were placed at room temperature for 4 hours, and the serum was collected by centrifugation and subjected to aspartate aminotransferase (AST) and alanine aminotransferase (ALT) assays following the manufacturer's protocols (Jiancheng Bioengineering Institute, Nanjing, China).

Determination of Triglyceride (TG) in Mouse Liver

Briefly, 20 mg of mouse liver tissues were added with 180 μl of homogenization solution (absolute ethanol) according to the ratio of weight (g): volume (ml) = 1:9, and homogenized mechanically on ice. Thereafter, homogenized tissues were centrifuged at 2500 rpm, 4 °C for 10 minutes. The supernatant was transferred and subjected to TG measurement using triglyceride assay kit (Jiancheng Bioengineering Institute, Nanjing, China) according to the manufacturer's instructions.

Histological Analysis and Evaluation of Lipid Accumulation in Mouse Liver

The mouse liver was washed several times with ice-cold 0.9% normal saline, fixed with 4% paraformaldehyde and embedded in paraffin wax. The liver paraffin sections (3 μm thick) were subjected to hematoxylin-eosin (H&E) staining using standard protocol, and examined under a digital microscope (Laica DM4000 B LED, Wetzlar, Germany). Frozen sections of liver (6μm thick) were stained with oil red O (ORO) to assess lipid accumulation under Laica DM4000 BLED microscope. Image J software (NIH, Bethesda, MD, USA) was employed for quantification.

Immunohistochemistry Assay

The levels of p-AMPK and ACC in mouse liver were evaluated by immunohistochemistry using an immunohistochemical staining kit (PV-9000, ZSBIO, Beijing, China). Briefly, liver paraffin sections (3 μm thick) were dewaxed and rehydrated with a gradient of xylene and a series of ethanol. A 0.01M sodium citrate buffer (ZLI-9064, ZSBIO, Beijing, China) with PH=6.0 was used for antigen thermal retrieval under a heating condition. After cooling, the sections were washed with PBS, incubated with endogenous peroxidase blocker for 20 minutes at room temperature, followed by blocking for 1 hour and primary antibody incubation using anti-rabbit Phospho-AMPKα (1:100, #2535, Cell Signaling Technology), anti-rabbit-ACC (1:200, #3676, Cell Signaling Technology) antibodies at 4°C overnight. Finally, the immunoreactivity was developed using freshly prepared DAB solution and counterstained with hematoxylin dye. After dehydration with alcohol, the sections were sealed with neutral gum, and examined under Laica DM4000 B LED microscope.

HepG2 Cell Culture and Treatment

HepG2 cells were provided by the Nerve Regeneration Laboratory, School of Medicine, Nantong University, and cultured in Dulbecco's modified Eagle's medium (DMEM; GIBCO, Shanghai, China) supplemented with10% heat-inactivated fetal bovine serum (FBS; GIBCO, Shanghai, China) in a humidity incubator containing 5% CO_2 at 37 °C. Cells with a confluency of 70-80% were exposed to different concentrations of PFOS (0, 50, 100 and 150 μM) dissolved in DMSO for 48 hours. The control group was treated with vehicle control (0.1% DMSO). As for AICAR treatment (M4869, AbMole, Shanghai, China), cells were pre-treated with 200μM AICAR for 1 hour, and then exposed to 150μM PFOS for 48 hours.

Cell Counting Kit-8 (CCK-8) Assay

Cell Counting Kit-8(CCK8, Biosharp, Shanghai, China) was employed to assess cell viability according to the manufacturer's instructions. HepG2 cells were seeded on the 96-well plates at a density of 7000 cells per well, and then exposed to different

concentrations (0, 25, 50, 100, 150and 200 μM) of PFOS for 24 hours after attaching. The medium was replaced with 10 μ CCK-8 solution and 90 μ DMEM complete medium, followed by incubation in a 37 °C incubator for 2 hours. Finally, the absorbance at 450nm was measured with a microplate reader (BioTek Elx800, Winusky, Vermont, U.S.). The experiment was repeated three times with similar results obtained.

Cell Oil Red O (ORO) Staining Analysis

HepG2 cells were cultured in a six-well plate and exposed to AICAR (200 μM) for 48 hours in the presence or absence of 150 μM PFOS. According to the instructions of the kit (Jiancheng Bioengineering Institute, Nanjing, China), the oil red dye solution was prepared and filtered using a filter paper. After aspirating the medium, wash with PBS, add the oil red dye solution to stain for 20 minutes, wash in 37 °C warm water, and then counter-stain the nucleus for 1 min. Observe and collect images under a microscope, and use Image J software for quantitative analysis.

Western Blot Analysis

The cell samples were lysed on ice with an appropriate amount of RIPA lysis buffer (P0013B, Beyotime, Shanghai, China) for 30 minutes, sonicate them, and centrifuged at 13000 rpm at 4 ℃ for 10 minutes. Take the supernatant and use the BCA protein concentration determination kit (P0010, Beyotime, Shanghai, China) to determine the protein concentration. The samples were electrophoresed in 6% or 10% sodium dodecyl sulfate-polyacrylamide gel (SDS-PAGE), then transferred to a PVDF membrane, and blocked with 5% BSA (BioFroxx, Einhausen, Germany) for 2 hours. Compared with rabbit anti-ACC (1:1000, #3676, CST), rabbit anti-Phospho AMPKα (1:1000, #2535, CST), rabbit anti-AMPKα (1:1000, #5831, CST), mouse After incubating with anti-GAPDH (1:6000, 60004-1-Ig, Proteintech) at 4℃overnight, TBST was washed and incubated with horseradish peroxidase (HRP) - bound secondary antibodies (1:6000, ab6721, Abcam) for 1 h at room temperature. Finally, using an enhanced chemiluminescence system (Tanon, Shanghai, China) to detect protein band. The quantification was performed by analyzing the gray value of Image J software (NIH,

Bethesda, MD, USA).

Statistical Analyses

All data are obtained from at least three independent experiments, and expressed in the form of mean±SEM. Two-way analysis of variance and one-way analysis of variance were used to evaluate the statistical differences of the results. $P<0.05$ was considered to be statistically significant. All statistical analyses were performed using IBM SPSS 22.0 software (IBM Corporation, Armonk, New York, USA).

RESULTS

PFOS Exposure Induced Liver Damage in Mice

In order to decipher the effect of PFOS exposure on liver lipid metabolism, a high-fat-diet (HFD)-induced liver steatosis model was established and administrated with different doses of PFOS. Mice were fed with Chow diet or HFD for 12 weeks, and given vehicle control, 1 mg/kg or 5 mg/kg PFOS on a daily basis in the last four weeks. We found that after the administration of PFOS, both Chow and HFD mice showed varying degrees of weight loss (Fig 1a and 1b), and signs of lethargy and dim coat. Compared with corresponding vehicle control groups, HFD plus 5 mg/kg PFOS group exhibited the most significant weight loss among all PFOS-exposed groups (Fig 1b). Meanwhile, PFOS exposure led to increased liver weights and liver-to-body ratios in both Chow and HFD groups (Fig 1c and 1d). By measuring the content of triglycerides in the liver of mice, it was found that PFOS exposure increased the accumulation of triglycerides in the liver of Chow and HFD mice (Fig 1e). PFOS exposure caused liver damage both in Chow and HFD mice, and high fat diet aggravated PFOS-induced liver damage, as revealed by serum levels of ALT and AST (Fig 1f and 1g). These data indicate that PFOS exposure may exacerbate HFD liver damage, particularly when combined with HFD.

PFOS Exposure Caused Lipid Accumulation in the Liver of Mice

Given the fact that PFOS exposure exacerbated HFD-induced liver TG accumulation, we evaluated the effect of PFOS treatment on liver lipid accumulation using oil red O staining and hematoxylin-eosin staining. As shown in Fig 2a, PFOS exposure caused fat vacuoles in the liver of mice, both in Chow and HFD-fed mice. In agreement, the oil red O staining results also pointed to a role of PFOS exposure in facilitating liver fat accumulation. In Chow-fed groups, PFOS exposure caused significant fat accumulation. Notably, PFOS exposure induced a higher degree of fat accumulation in HFD group than Chow group (Fig 2b and 2c). In addition, transmission electron microscopy (TEM) analysis found that PFOS exposure induced fatty vacuoles in the liver of mice, and PFOS exposure-induced liver fat accumulation was more pronounced in mice fed a high-fat diet (HFD group) than in the Chow group (Fig 2d). These findings infer that PFOS induces liver fat accumulation and may aggravate liver steatosis in HFD mice.

AMPK Played an Important Role in PFOS-Induced Liver Steatosis

Mounting data indicate that AMPK plays a vital role in lipid metabolism and the regulation of liver steatosis. In order to explore a role of AMPK in PFOS-induced liver lipid metabolic disorders, we used immunohistochemical staining to detect the expression of phosphorylated AMPK in the liver of Chow and HFD groups (Fig 3a). We found that compared with mock-exposed groups, PFOS exposure led to reduced expression of p-AMPK, especially in HFD groups (Fig 3b). This result suggests that PFOS exposure inhibits the phosphorylation of AMPK, which plays an important role in PFOS-induced fat accumulation.

PFOS Inhibits AMPK Activation in HepG2 Cells

In order to verify the results of in vivo experiments, we used HepG2 cells to establish a PFOS exposure model in vitro. HepG2 cells were exposed to different concentrations of PFOS for 24 hours, and subjected to cytotoxic assay using a CCK-8 kit (Fig 4a). We found that treatment with 200μM PFOS caused cell viability decrease by 45%, while mild decrease in viability and no morphological changes were observed

in HepG2 cells exposed to lower doses of PFOS. Therefore, in follow-up experiments, we use 0, 50, 100 and 150μM PFOS for experiments. As predicted, western blot results showed that the expression of p-AMPK declined in a concentration-dependent manner, while the total protein level of AMPK was unchanged (Figure 4b and 4d). ACC acts as a key downstream effector of AMPK-mediated lipid metabolism. Reduced AMPK activity can directly lead to reduced level of ACC phosphorylation, which in turn enhances the activity of ACC and promotes fat accumulation. Thus, consistently, Western blot results indicated that the expression of p-ACC also decreased in a concentration-dependent manner, while the total protein level of ACC remained relatively unchanged (Figure 4b and 4c). At the same time, by staining with Oil Red O, we found that after exposure to PFOS, significant lipid accumulation appeared in HepG2 cells (Fig 5b). The above data all suggest that PFOS may inhibit cellular β-oxidation and induce fat accumulation by inhibiting the phosphorylation of AMPK ACC.

Intervention with AMPK Agonist Blocks PFOS-Induced Lipid Accumulation

Next, in order to further decipher a causal role of AMPK activity in aberrant lipid metabolism following PFOS exposure, AMPK agonist AICAR was employed to verify whether agonizing AMPK can reverse PFOS-induced lipid accumulation. HepG2 cells were exposed to AICAR (200 μM) in the presence or absence of 150 μM PFOS for 48 hours. Western blot results showed that the intervention treatment of AICAR significantly increased the expression of phosphorylated ACC (Fig 5a). In addition, the results of Oil Red O showed that phosphorylation activation of AMPK significantly alleviated PFOS-induced fat accumulation in HepG2 cells (Fig 5b). Taken together, these findings implicated that AMPK plays a key role in PFOS-induced liver steatosis.

DISCUSSION

Mounting data from epidemiological and animal studies have confirmed an involvement of PFOS exposure on liver damage and metabolic disorder (Berthiaume and Wallace 2002; Cui et al. 2017; Geng et al. 2019; Liu et al. 2007; Marques et al.

2020). In this research, through establishing a mouse model of HFD-induced liver fat accumulation, we found that PFOS inhibited the activation of AMPK and enhanced the activity of ACC. Using western blotting analysis, we found that PFOS reduced the level of phosphorylated AMPK, while the total amount of AMPK was largely unchanged. In addition, we have also found in mouse animal experiments that high-fat diet increased the degree of PFOS-induced liver fat accumulation, and there may be a synergistic effect between HFD and PFOS in inducing liver lipid accumulation.

The development of liver steatosis is mainly attributed to disorders in liver lipid metabolism. While aberrant lipid metabolism plays an integral role in liver fat accumulation, the involvement of other factors, such as toxicant exposure and inflammation, cannot be neglected. Indeed, exposure to various environmental pollutants, including 2,3,7,8-tetrachlorodibenzofuran (TCDF), Benzo[a]pyrene and diesel exhaust, has been shown to cause liver steatosis (Feng et al. 2020; Yin et al. 2019; Yuan et al. 2020). Exposure to high doses of PFOS (10 mg/kg) has been also reportedly associated with the development of steatosis (Wan et al. 2012). However, this dose range is pretty high and physiologically irrelevant. In addition, the development of steatosis is typically driven by multiple factors, including genetic predisposition, excess energy intake and toxicant-induced hepatic damage. On the basis of the hypothesis that PFOS exposure may work synergically with nutritional factors to facilitate hepatic steatosis, we established a HFD-induced steatosis model and investigated the synergic effects of PFOS and HFD in facilitating steatosis. We found that 1mg/kg PFOS significantly aggravated HFD-induced steatosis, as revealed by histological and biochemical data. These results suggested that PFOS bioaccumulation may be a risk factor of steatosis, particularly in subjects with excess fat intake.

As a master regulator of energy metabolism, AMPK also plays an indispensable role in balancing lipid catabolism and synthesis. Studies in recent years revealed that AMPK-activating therapies and drugs may provide significant benefits in the prevention of metabolic associated fatty liver disease (MAFLD) (Chen et al. 2019; Li et al. 2011; Smith et al. 2016; Zhu et al. 2019). These results are consistent with the notion that aberrant AMPK activity plays a causal role in the development of MAFLD.

Therefore, we believe that PFOS-induced inactivation of AMPK may contribute heavily to the accumulation of fat in the liver. In line with our data that PFOS may attenuate the activity of AMPK, a recent report also showed that PFOS can hinder the hypoglycemic effect of metformin (an AMPK agonist) (Salter et al. 2021). In our experiments, we also observed that PFOS can reduce the phosphorylation of AMPK. Once AMPK is inactivated, the activity of ACC will increase accordingly, thereby promoting fatty acid synthesis (Assifi et al. 2005; Carling et al. 1987; Munday et al. 1988). We also found that pretreatment with AMPK agonist AICAR can reduce PFOS-mediated lipid accumulation in the liver. This further indicates that PFOS mediates liver steatosis through AMPK/ACC. In addition, acute exposure to PFOS increases insulin secretion (Zhang et al. 2020), and the insulin/IGF-1 signaling pathway inhibits the activation of AMPK (Hawley et al. 2014; Horman et al. 2006; Kovacic et al. 2003; Ning et al. 2011). We speculate that the insulin pathway-mediated AMPK inactivation may serve as an indirect mechanism leading to PFOS-induced lipid accumulation.

In summary, our study verified a role of aberrant AMPK activity in PFOS-induced liver lipid accumulation, and dissected the mechanism by which AMPK-ACC pathway contributes to PFOS-induced lipid accumulation. PFOS inhibits the phosphorylation of AMPK, promotes the expression of ACC, and inhibits the oxidation of fatty acid β, which leads to the accumulation of lipids in the liver and the development of MAFLD. This study provides new insights for elucidating the mechanism underpinning PFOS-induced liver fat metabolism, and also provides a new theoretical basis for preventing and intervening PFOS liver toxicity.

REFERENCES

Assifi MM, Suchankova G, Constant S, Prentki M, Saha AK, Ruderman NB (2005) AMP-activated protein kinase and coordination of hepatic fatty acid metabolism of starved/carbohydrate-refed rats. American journal of physiology Endocrinology and metabolism 289(5):E794-800 doi:10.1152/ajpendo.00144.2005

Bach CC, Bech BH, Brix N, Nohr EA, Bonde JP, Henriksen TB (2015) Perfluoroalkyl and polyfluoroalkyl substances and human fetal growth: a systematic review. Crit Rev Toxicol 45(1):53-67 doi:10.3109/10408444.2014.952400

Berthiaume J, Wallace KB (2002) Perfluorooctanoate, perflourooctanesulfonate, and N-ethyl perfluorooctanesulfonamido ethanol; peroxisome proliferation and mitochondrial biogenesis. Toxicology letters 129(1-2):23-32 doi:10.1016/s0378-4274(01)00466-0

Carling D, Zammit VA, Hardie DG (1987) A common bicyclic protein kinase cascade inactivates the regulatory enzymes of fatty acid and cholesterol biosynthesis. FEBS letters 223(2):217-22 doi:10.1016/0014-5793(87)80292-2

Chen XY, Cai CZ, Yu ML, et al. (2019) LB100 ameliorates nonalcoholic fatty liver disease via the AMPK/Sirt1 pathway. World journal of gastroenterology 25(45):6607-6618 doi:10.3748/wjg.v25.i45.6607

Cui Y, Lv S, Liu J, et al. (2017) Chronic perfluorooctanesulfonic acid exposure disrupts lipid metabolism in zebrafish. Human & experimental toxicology 36(3):207-217 doi:10.1177/0960327116646615

Fang K, Wu F, Chen G, et al. (2019) Diosgenin ameliorates palmitic acid-induced lipid accumulation via AMPK/ACC/CPT-1A and SREBP-1c/FAS signaling pathways in LO2 cells. BMC Complement Altern Med 19(1):255 doi:10.1186/s12906-019-2671-9

Feng D, Zhang H, Jiang X, et al. (2020) Bisphenol A exposure induces gut microbiota dysbiosis and consequent activation of gut-liver axis leading to hepatic steatosis in CD-1 mice. Environmental pollution (Barking, Essex : 1987) 265(Pt A):114880 doi:10.1016/j.envpol.2020.114880

Geng D, Musse AA, Wigh V, et al. (2019) Effect of perfluorooctanesulfonic acid (PFOS) on the liver lipid metabolism of the developing chicken embryo. Ecotoxicology and environmental safety 170:691-698 doi:10.1016/j.ecoenv.2018.12.040

Giesy JP, Kannan K (2001) Global distribution of perfluorooctane sulfonate in wildlife. Environmental science & technology 35(7):1339-42 doi:10.1021/es001834k

Gleason JA, Post GB, Fagliano JA (2015) Associations of perfluorinated chemical serum concentrations and biomarkers of liver function and uric acid in the US population (NHANES), 2007-2010. Environmental research 136:8-14 doi:10.1016/j.envres.2014.10.004

Han R, Zhang F, Wan C, Liu L, Zhong Q, Ding W (2018) Effect of perfluorooctane sulphonate-induced Kupffer cell activation on hepatocyte proliferation through the NF-kappaB/TNF-alpha/IL-6-dependent pathway. Chemosphere 200:283-294 doi:10.1016/j.chemosphere.2018.02.137

Hawley SA, Ross FA, Gowans GJ, Tibarewal P, Leslie NR, Hardie DG (2014) Phosphorylation by Akt within the ST loop of AMPK-α1 down-regulates its activation in tumour cells. The Biochemical journal 459(2):275-87 doi:10.1042/bj20131344

Herzig S, Shaw RJ (2018) AMPK: guardian of metabolism and mitochondrial homeostasis. Nature reviews Molecular cell biology 19(2):121-135 doi:10.1038/nrm.2017.95

Horman S, Vertommen D, Heath R, et al. (2006) Insulin antagonizes ischemia-induced Thr172 phosphorylation of AMP-activated protein kinase alpha-subunits in heart via hierarchical phosphorylation of Ser485/491. The Journal of biological chemistry 281(9):5335-40 doi:10.1074/jbc.M506850200

Huang T, Zhang Y, Zhang W, et al. (2020) Attenuation of Perfluorooctane Sulfonate-Induced Steatohepatitis by Grape Seed Proanthocyanidin Extract in Mice. BioMed research international 2020:8818160 doi:10.1155/2020/8818160

Kim MK, Kim SH, Yu HS, et al. (2012) The effect of clozapine on the AMPK-ACC-CPT1 pathway in the rat frontal cortex. The international journal of neuropsychopharmacology 15(7):907-17 doi:10.1017/s1461145711000976

Kovacic S, Soltys CL, Barr AJ, Shiojima I, Walsh K, Dyck JR (2003) Akt activity negatively regulates phosphorylation of AMP-activated protein kinase in the heart. The Journal of biological chemistry 278(41):39422-7 doi:10.1074/jbc.M305371200

Lane MD, Wolfgang M, Cha SH, Dai Y (2008) Regulation of food intake and energy expenditure by hypothalamic malonyl-CoA. International journal of obesity (2005) 32 Suppl 4:S49-54 doi:10.1038/ijo.2008.123

Lau C, Butenhoff JL, Rogers JM (2004) The developmental toxicity of perfluoroalkyl acids and their derivatives. Toxicol Appl Pharmacol 198(2):231-41 doi:10.1016/j.taap.2003.11.031

Li Y, Xu S, Mihaylova MM, et al. (2011) AMPK phosphorylates and inhibits SREBP activity to attenuate hepatic steatosis and atherosclerosis in diet-induced insulin-resistant mice. Cell metabolism 13(4):376-388 doi:10.1016/j.cmet.2011.03.009

Lindstrom AB, Strynar MJ, Libelo EL (2011) Polyfluorinated compounds: past, present, and future. Environmental science & technology 45(19):7954-61 doi:10.1021/es2011622

Liu B, Zhang H, Xie L, et al. (2015) Spatial distribution and partition of perfluoroalkyl acids (PFAAs) in rivers of the Pearl River Delta, southern China. The Science of the total environment 524-525:1-7 doi:10.1016/j.scitotenv.2015.04.004

Liu C, Yu K, Shi X, et al. (2007) Induction of oxidative stress and apoptosis by PFOS and PFOA in primary cultured hepatocytes of freshwater tilapia (Oreochromis niloticus). Aquatic toxicology (Amsterdam, Netherlands) 82(2):135-43 doi:10.1016/j.aquatox.2007.02.006

Maestri L, Negri S, Ferrari M, et al. (2006) Determination of perfluorooctanoic acid and perfluorooctanesulfonate in human tissues by liquid chromatography/single quadrupole mass spectrometry. Rapid communications in mass spectrometry : RCM 20(18):2728-34 doi:10.1002/rcm.2661

Marques E, Pfohl M, Auclair A, et al. (2020) Perfluorooctanesulfonic acid (PFOS) administration shifts the hepatic proteome and augments dietary outcomes related to hepatic steatosis in mice. Toxicol Appl Pharmacol 408:115250 doi:10.1016/j.taap.2020.115250

McDonough CA, Ward C, Hu Q, Vance S, Higgins CP, DeWitt JC (2020) Immunotoxicity of an Electrochemically Fluorinated Aqueous Film-Forming Foam. Toxicological sciences : an official journal of the Society of Toxicology 178(1):104-114 doi:10.1093/toxsci/kfaa138

Miralles-Marco A, Harrad S (2015) Perfluorooctane sulfonate: a review of human exposure, biomonitoring and the environmental forensics utility of its chirality and isomer distribution. Environ Int 77:148-59 doi:10.1016/j.envint.2015.02.002

Munday MR, Campbell DG, Carling D, Hardie DG (1988) Identification by amino acid sequencing of three major regulatory phosphorylation sites on rat acetyl-CoA carboxylase. European journal of biochemistry 175(2):331-8 doi:10.1111/j.1432-1033.1988.tb14201.x

Ning J, Xi G, Clemmons DR (2011) Suppression of AMPK activation via S485 phosphorylation by IGF-I during hyperglycemia is mediated by AKT activation in vascular smooth muscle cells. Endocrinology 152(8):3143-54 doi:10.1210/en.2011-0155

Olsen GW, Hansen KJ, Stevenson LA, Burris JM, Mandel JH (2003) Human donor liver and serum concentrations of perfluorooctanesulfonate and other perfluorochemicals. Environmental science & technology 37(5):888-91 doi:10.1021/es020955c

Olsen GW, Zobel LR (2007) Assessment of lipid, hepatic, and thyroid parameters with serum perfluorooctanoate (PFOA) concentrations in fluorochemical production workers. International archives of occupational and environmental health 81(2):231-46 doi:10.1007/s00420-007-0213-0

Pan CH, Tsai CH, Lin WH, Chen GY, Wu CHJE-BC, Medicine A (2012) Ethanolic Extract of Vitis thunbergii Exhibits Lipid Lowering Properties via Modulation of the AMPK-ACC Pathway in Hypercholesterolemic Rabbits. 2012:1-10

Perez F, Nadal M, Navarro-Ortega A, et al. (2013) Accumulation of perfluoroalkyl substances in human tissues. Environ Int 59:354-62 doi:10.1016/j.envint.2013.06.004

Pollutants SJhcpiCPCGMtle-UDa (2009) Governments unite to step-up reduction on global DDT reliance and add nine new chemicals under international treaty.

Qiang X, Xu L, Zhang M, et al. (2016) Demethyleneberberine attenuates non-alcoholic fatty liver disease with activation of AMPK and inhibition of oxidative stress.603-609

Riebe RA, Falk S, Georgii S, Brunn H, Failing K, Stahl T (2016) Perfluoroalkyl Acid Concentrations in Livers of Fox (Vulpes vulpes) and Chamois (Rupicapra rupicapra) from Germany and Austria. Archives of environmental contamination and toxicology 71(1):7-15 doi:10.1007/s00244-015-0250-8

Salter DM, Wei W, Nahar PP, Marques E, Slitt AL (2021) Perfluorooctanesulfonic Acid (PFOS) Thwarts the Beneficial Effects of Calorie Restriction and Metformin. Toxicological sciences : an official journal of the Society of Toxicology 182(1):82-95 doi:10.1093/toxsci/kfab043

Schreurs M, Kuipers F, van der Leij FR (2010) Regulatory enzymes of mitochondrial beta-oxidation as targets for treatment of the metabolic syndrome. Obesity reviews : an official journal of the International Association for the Study of Obesity 11(5):380-8 doi:10.1111/j.1467-789X.2009.00642.x

Smith BK, Marcinko K, Desjardins EM, Lally JS, Ford RJ, Steinberg GR (2016) Treatment of nonalcoholic fatty liver disease: role of AMPK. American journal of physiology Endocrinology and metabolism 311(4):E730-e740 doi:10.1152/ajpendo.00225.2016

Wan HT, Zhao YG, Wei X, Hui KY, Giesy JP, Wong CK (2012) PFOS-induced hepatic steatosis, the mechanistic actions on beta-oxidation and lipid transport. Biochim Biophys Acta 1820(7):1092-101 doi:10.1016/j.bbagen.2012.03.010

Wang L, Wang Y, Liang Y, et al. (2014) PFOS induced lipid metabolism disturbances in BALB/c mice through inhibition of low density lipoproteins excretion. Scientific reports 4:4582 doi:10.1038/srep04582

Yin F, Gupta R, Vergnes L, et al. (2019) Diesel Exhaust Induces Mitochondrial Dysfunction, Hyperlipidemia, and Liver Steatosis. Arteriosclerosis, thrombosis, and vascular biology 39(9):1776-1786 doi:10.1161/atvbaha.119.312736

You M, Matsumoto M, Pacold CM, Cho WK, Crabb DW (2004) The role of AMP-activated protein kinase in the action of ethanol in the liver. Gastroenterology 127(6):1798-808 doi:10.1053/j.gastro.2004.09.049

Yuan P, Dong M, Lei H, et al. (2020) Targeted metabolomics reveals that 2,3,7,8-tetrachlorodibenzofuran exposure induces hepatic steatosis in male mice. Environmental pollution (Barking, Essex : 1987) 259:113820 doi:10.1016/j.envpol.2019.113820

Zhang L, Duan X, Sun W, Sun H (2020) Perfluorooctane sulfonate acute exposure stimulates insulin secretion via GPR40 pathway. The Science of the total environment 726:138498 doi:10.1016/j.scitotenv.2020.138498

Zhu X, Bian H, Wang L, et al. (2019) Berberine attenuates nonalcoholic hepatic steatosis through the AMPK-SREBP-1c-SCD1 pathway. Free radical biology & medicine 141:192-204 doi:10.1016/j.freeradbiomed.2019.06.019

ACKNOWLEDGMENTS

This study was supported by the National Natural Science Foundation of China (no. 81902406), Nantong Science and Technology Project (JC2020032) and Taizhou people's hospital research project (ZL201916).

CONFLICT OF INTEREST STATEMENT

The authors declare no conflict of interest.

Figure Legends

Fig 1 PFOS exposure induces liver injury in C57BL/6 mice

Mice were fed chow diet (Chow) or high-fat diet (HFD) for 12 weeks, and were administered 1 mg/kg, 5 mg/kg PFOS or vehicle carrier (corn oil) in the last 4 weeks. The body weight (BW) changes of 4-week-old mice fed for 12 weeks in Chow group (**a**) and HFD group (**b**). We also assessed the (**c**) liver weight, (**d**) liver organ coefficient, (**e**) liver triglyceride (TG) content, (**f**) serum alanine aminotransferase (ALT) and (**g**) aspartate aminotransferase (AST) content. Note: Values are mean ± SEM. *, $P<0.05$, VS Con group (A and B); &, $P<0.05$, VS Chow-Con group; #, $P<0.05$, VS HFD-Con group; *, $P<0.05$, VS Chow group.

Fig 2 PFOS exposure induces liver steatosis in mice

(**a**) H&E staining analysis of liver tissue sections. Scale bar: 50μm. (**b**) Oil red O staining analysis of mouse liver tissue sections. Scale bar: 50μm. (**c**) Histogram of quantitative analysis of oil red O staining results. (**d**) Transmission electron microscopy analysis of mouse liver tissue sections. Scale bar: 0.5μm. Note: Values are mean ± SEM. &, $P<0.05$, VS Chow-Con group; #, $P<0.05$, VS HFD-Con group; *, $P<0.05$, VS Chow group.

Fig 3 PFOS exposure reduces the levels of phosphorylated AMPK in the liver of mice

(**a**) Immunohistochemistrical analysis of the expression of phosphorylated AMPK in liver tissue sections of mice in each experimental group. Scale bar: 50μm. (**b**) Histogram of positive results for quantitative analysis of p-AMPK in mouse liver. Note:

Values are mean ± SEM. &, P<0.05, VS Chow-Con group; #, P<0.05, VS HFD-Con group; *, P<0.05, VS Chow group.

Fig 4 Effect of PFOS exposure on AMPK/ACC signaling in HepG2 cells

HepG2 cells were treated with different concentrations of PFOS (0, 50, 100 and 150 μM) for 48 hours. (**a**) Analysis of cell viability by CCK-8 detection method. (**b**) Expression analysis of p-ACC, ACC, p-AMPK and AMPK in HepG2 cells. (**c**) Histogram means the density ratio of p-ACC/ACC. (**d**) Histogram denotes the density ratio of p-AMPK/AMPK. Note: Values are mean ± SEM. *, P<0.05.

Fig 5 AMPK activation can alleviate the fat accumulation of HepG2 cells induced by PFOS exposure

HepG2 cells were exposed to AICAR (200 μM) in the presence or absence of 150 μM PFOS for 48 hours. (**a**) The expression of p-ACC and ACC in HepG2 cells was analyzed by Western blot. The histogram shows the density ratio of p-ACC/ACC. (**b**) Oil red O staining analysis. Scale bar: 50μm. The histogram represents the quantitative analysis of the oil red O staining results. Note: Values are mean ± SEM. *, P<0.05.

Figures

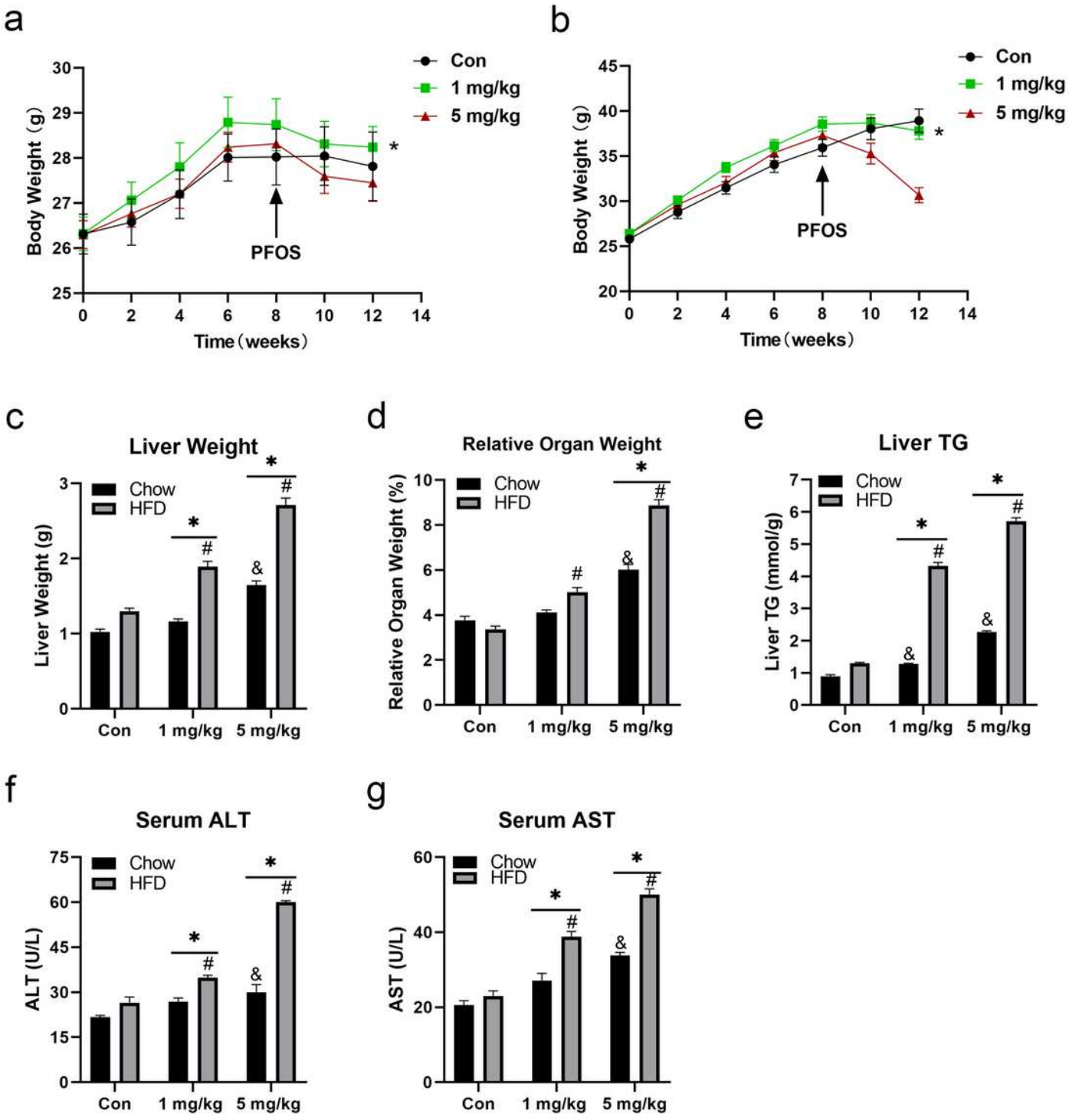

Figure 1

PFOS exposure induces liver injury in C57BL/6 mice

Mice were fed chow diet (Chow) or high-fat diet (HFD) for 12 weeks, and were administered 1 mg/kg, 5 mg/kg PFOS or vehicle carrier (corn oil) in the last 4 weeks. The body weight (BW) changes of 4-week-old mice fed for 12 weeks in Chow group (a) and HFD group (b). We also assessed the (c) liver weight, (d) liver organ coefficient, (e) liver triglyceride (TG) content, (f) serum alanine aminotransferase (ALT) and (g) aspartate aminotransferase (AST) content. Note: Values are mean ± SEM. *, P<0.05, VS Con group (A and B); &, P<0.05, VS Chow-Con group; #, P<0.05, VS HFD-Con group; *, P<0.05, VS Chow group.

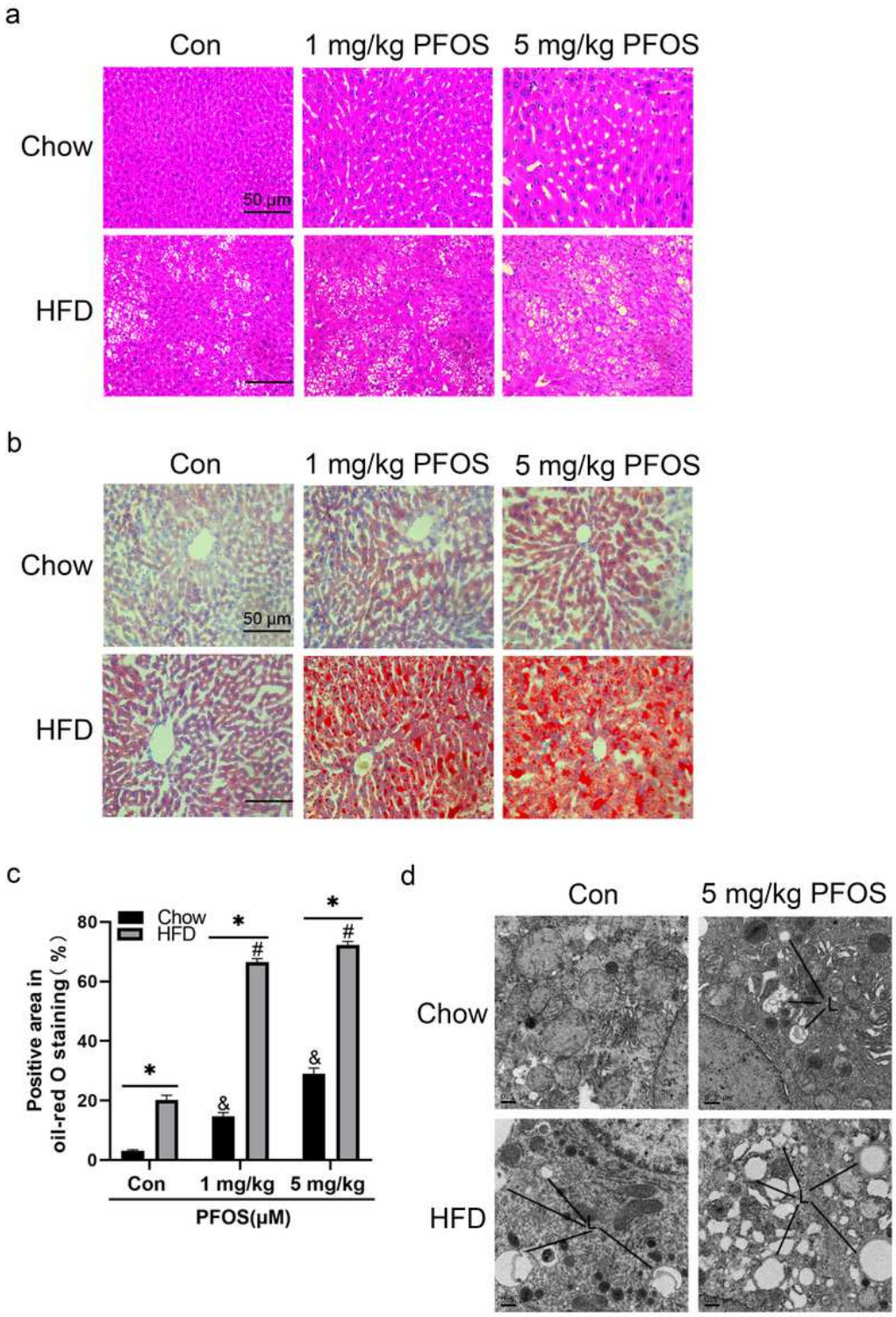

Figure 2

PFOS exposure induces liver steatosis in mice

(a) H&E staining analysis of liver tissue sections. Scale bar: 50μm. (b) Oil red O staining analysis of mouse liver tissue sections. Scale bar: 50μm. (c) Histogram of quantitative analysis of oil red O staining results. (d) Transmission electron microscopy analysis of mouse liver tissue sections. Scale bar: 0.5μm. Note: Values are mean ± SEM. &, P<0.05, VS Chow-Con group; #, P<0.05, VS HFD-Con group; *, P<0.05, VS Chow group.

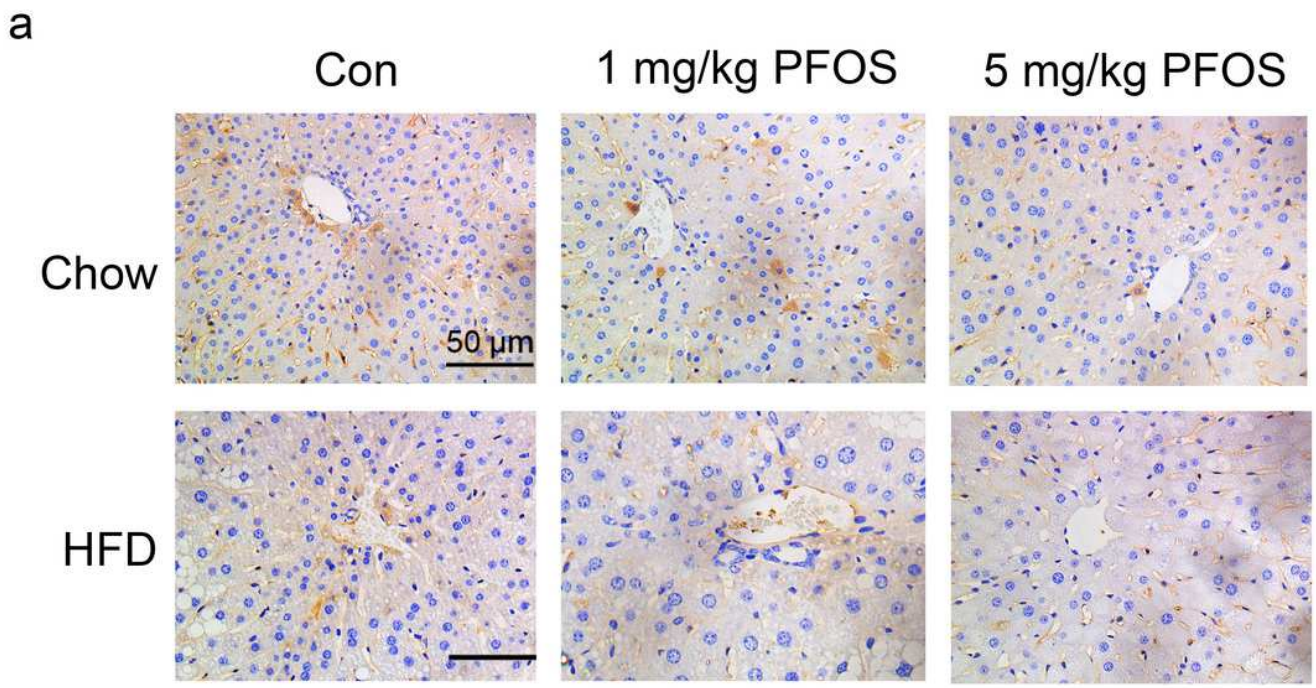

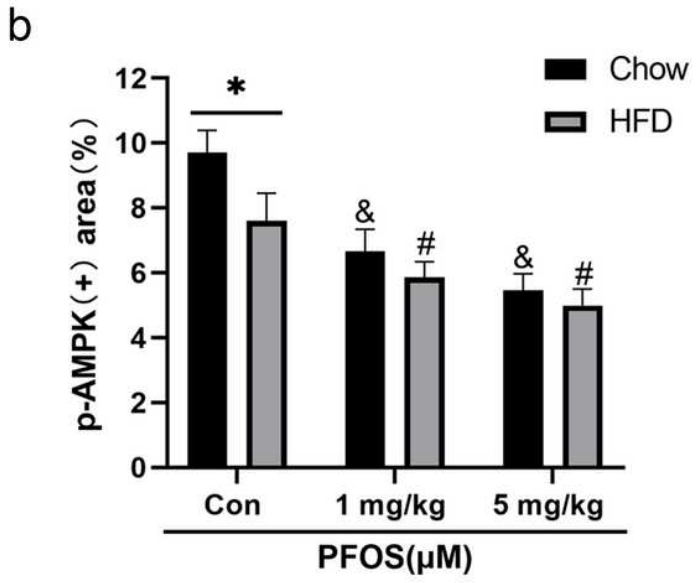

Figure 3

PFOS exposure reduces the levels of phosphorylated AMPK in the liver of mice

(a) Immunohistochemistrical analysis of the expression of phosphorylated AMPK in liver tissue sections of mice in each experimental group. Scale bar: 50μm. (b) Histogram of positive results for quantitative analysis of p-AMPK in mouse liver. Note:

Values are mean ± SEM. &, P<0.05, VS Chow-Con group; #, P<0.05, VS HFD-Con group; *, P<0.05, VS Chow group.

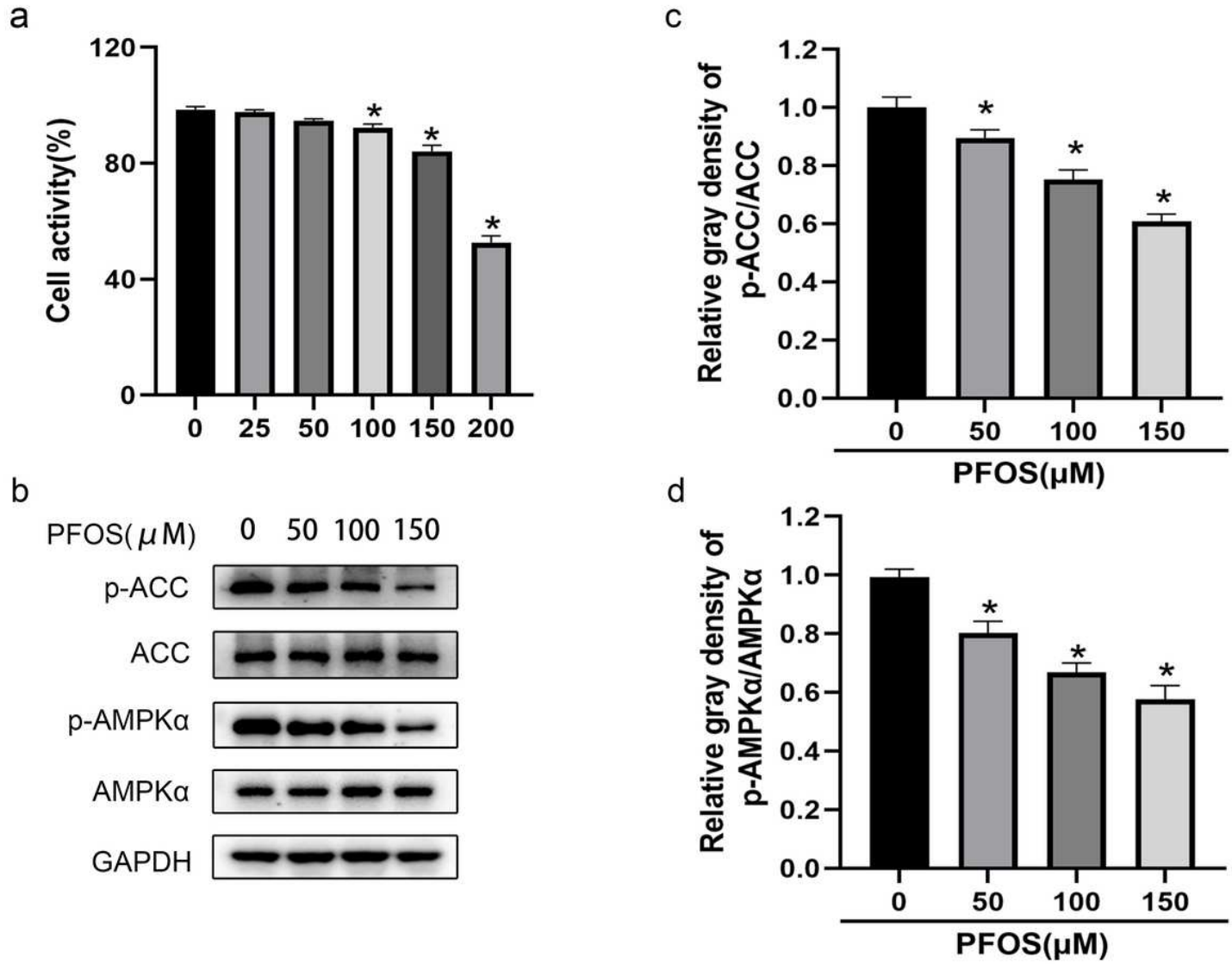

Figure 4

Effect of PFOS exposure on AMPK/ACC signaling in HepG2 cells

HepG2 cells were treated with different concentrations of PFOS (0, 50, 100 and 150 μM) for 48 hours. (a) Analysis of cell viability by CCK-8 detection method. (b) Expression analysis of p-ACC, ACC, p-AMPK and

AMPK in HepG2 cells. (c) Histogram means the density ratio of p-ACC/ACC. (d) Histogram denotes the density ratio of p-AMPK/AMPK. Note: Values are mean ± SEM. *, P<0.05.

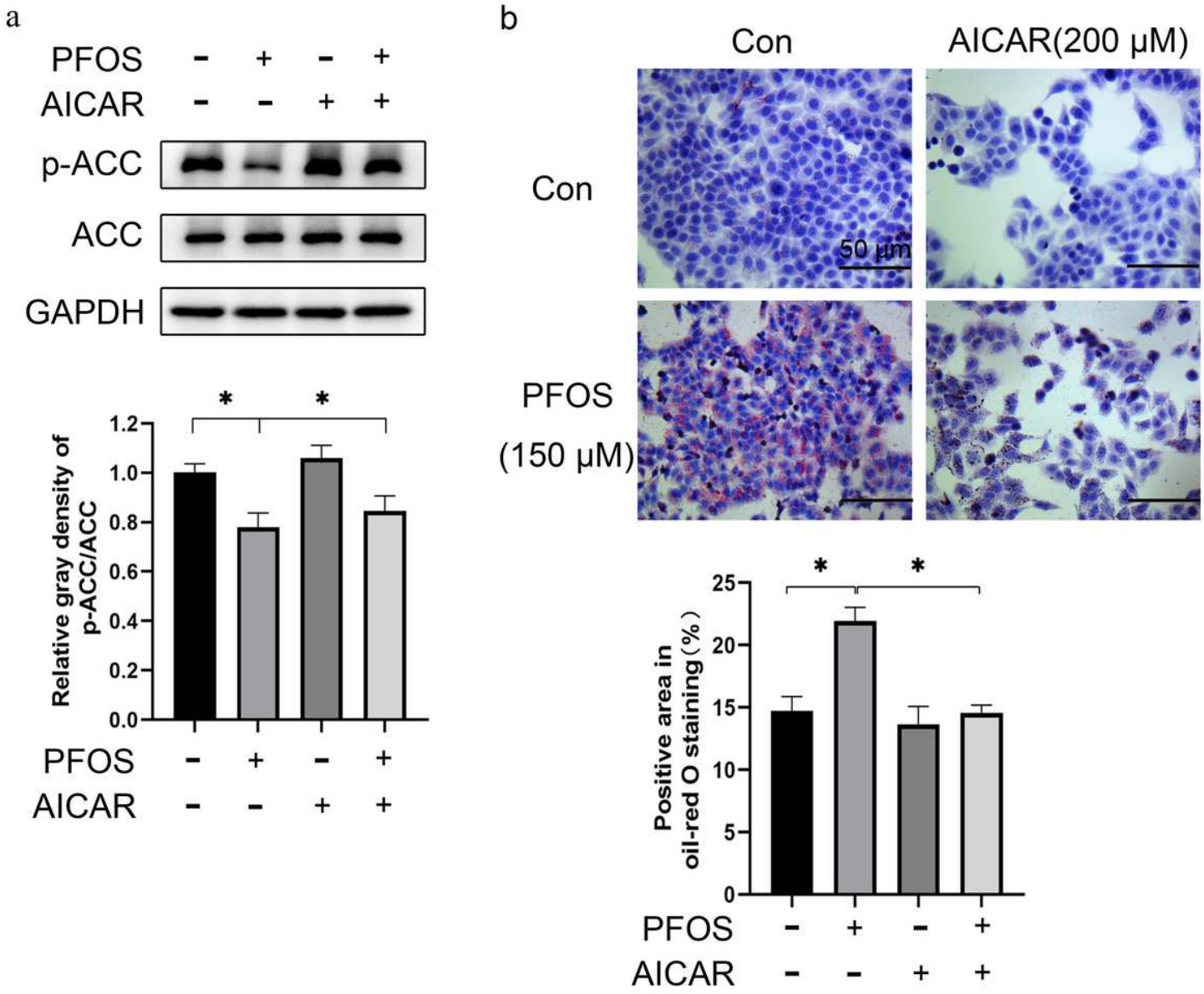

Figure 5

AMPK activation can alleviate the fat accumulation of HepG2 cells induced by PFOS exposure

HepG2 cells were exposed to AICAR (200 μM) in the presence or absence of 150 μM PFOS for 48 hours. (a) The expression of p-ACC and ACC in HepG2 cells was analyzed by Western blot. The histogram shows the density ratio of p-ACC/ACC. (b) Oil red O staining analysis. Scale bar: 50μm. The histogram represents the quantitative analysis of the oil red O staining results. Note: Values are mean ± SEM. *, P<0.05.